8th Biennial International Conference
& Exposition on Petroleum Geophysics

"HYDERABAD 2010"

P-85

The phase congruency algorithm – A carbonate case study

Brian Russell[1*], Dan Hampson[1], and John Logel[2]
[1] *Hampson-Russell, A CGGVeritas Company, Calgary, Alberta*
[2] *Talisman Energy Inc, Calgary, Alberta,*

Summary

The two-dimensional phase congruency algorithm using the log Gabor transform as developed by Kovesi (2003) is used to look for features such as edges and corners on two-dimensional images. In image processing, the algorithm has applications to robot vision and feature enhancement. In seismic analysis, we also look for features on 3D seismic cubes, but the features we look for are structural in nature. We implemented the Kovesi algorithm in a seismic analysis and display program. In our implementation, we use this algorithm to look for faults and fractures on slices taken from 3D seismic volumes. We illustrate this technique using a karst collapse study.

Introduction

Traditionally, the analysis of seismic data involved looking for continuous events on seismic data, from which structural and stratigraphic features could be mapped. However, we are also interested in mapping discontinuous features such as faults and fractures. A method for identifying these discontinuities was first introduced by Bahorich and Farmer (1995) and called the coherency algorithm. This method, based on cross-correlation between adjacent traces, has remained the industry standard since its introduction and has undergone several major enhancements.

However, researchers in other areas of image analysis, such as robot vision and feature identification, have also been developing ways to identify discontinuities on their images. One such development is the phase congruency algorithm (Kovesi, 2003), which is able to identify corners and edges on images of shapes and possible obstacles to enhance robot vision. In this paper, we have implemented the phase congruency algorithm in a seismic analysis toolbox and apply it to seismic data slices to look for discontinuities on these slices. We will then apply the method to a seismic volume recorded over a karst collapse feature.

Theory of Phase Congruency

The phase congruency (PC) algorithm was developed to detect corners and edges on 2D digital images (Kovesi, 2003). To understand the concept behind phase congruency in 2D space, with x and y coordinates, it is instructive to first understand the algorithm in 1D, with simply an x coordinate. Kovesi (2003) shows that a simple measure of phase congruency is given by

$$PC(x) = \frac{|E(x)|}{\sum_n A_n(x)} = \frac{\sum_n A_n(x)\cos(\phi_n(x) - \bar{\phi}(x))}{\sum_n A_n(x)} \quad (1)$$

where $A_n(x)$ and $\phi_n(x)$ are the length and phase angle of each of the individual n amplitude vectors, and $E(x)$ and $\bar{\phi}(x)$ are the length and phase angle of the summed vectors.

Kovesi (2003) then gives a more advanced formula that builds in a weight factor for frequency spread and a noise threshold. However, equation (1) is sufficient for an understanding of the basic algorithm. More importantly, Kovesi (2003) shows how to extend equation (1) to the two-dimensional image domain. This is done using oriented 2D Gabor wavelets in the 2D Fourier domain. In the initial implementation, Kovesi used 2D Gaussian

brian.russell@cggveritas.com, dan.hampson@cggveritas.com, jlogel@talisman-energy.com

wavelets, but in a later implementation he used log Gabor wavelets, as introduced by Field (1987). The advantage of the log Gabor transform when used for the radial filtering is that it is Gaussian on a logarithmic scale and thus has better high frequency characteristics than the traditional Gabor transform (Cook et al., 2006).

The first steps in the 2D phase congruency algorithm are to transform the data to the 2D Fourier domain, then apply *N*M* filters (*N* radial log Gabor filters multiplied by *M* angular filters). The log Gabor filters are computed over *N* "scales" *S*, where *S* = 0, … , *N*-1. Typically, the value of *N* is between 4 and 8. Each log Gabor filter is computed by the formula

$$\log Gabor_S = \exp\left[\frac{-\ln(r\cdot\lambda_S)^2}{\sigma}\right]\cdot lp, \qquad (2)$$

where r = the radius value from the zero frequency value, λ_S is the scale value, where $\lambda_S = 3m^S$, with a default value of m = 2.1, $\sigma = 2\ln(0.55)^2$ and lp is a low pass 2D Butterworth filter. The angular filters are created over M orientations or angles θ, where $\theta = 0, \pi/M, \ldots, (M\text{-}1)\pi/M$. The default value of M is 6, in which case the angles will go from 0^o to 150^o in increments of 30^o.

After the *N*M* filters are applied, each filtered image is transformed back to the spatial domain and, after appropriate weighting and noise thresholding, are summed over the scales to produce an image at each orientation. These images are then analyzed using moment analysis which, as described by Kovesi (2003) is equivalent to performing singular value decomposition on the phase congruency covariance matrix. In moment analysis terms, the maximum moment M and minimum moment m (which correspond to the singular values) are computed as follows:

$$M = \frac{1}{2}\left(c + a + \sqrt{b^2 + (a-c)^2}\right), \text{ and} \qquad (3)$$

$$m = \frac{1}{2}\left(c + a - \sqrt{b^2 + (a-c)^2}\right), \text{ where} \qquad (4)$$

$$a = \sum_{\theta=\theta_0}^{\theta_M}(PC(\theta)\cos\theta)^2,\ b = 2\sum_{\theta=\theta_0}^{\theta_M}[(PC(\theta)\cos\theta)(PC(\theta)\sin\theta)],$$

$$c = \sum_{\theta=\theta_0}^{\theta_M}(PC(\theta)\sin\theta)^2 .$$

According to Kovesi (2003), the interpretations of the maximum and minimum moments, which are the final results, are as follows. The magnitude of the maximum moment indicates the significance of a feature on the image, or its "edge". The magnitude of the minimum moment gives an indication of a "corner". In this study, we will only display the maximum moment M, since we are interested in edges.

A simple schematic diagram showing the way in which the phase congruency method was implemented on seismic data is shown in Figure 1. Although this algorithm proceeds by analyzing constant time slices, it should also be possible to apply the algorithm to structural or stratigraphic slices.

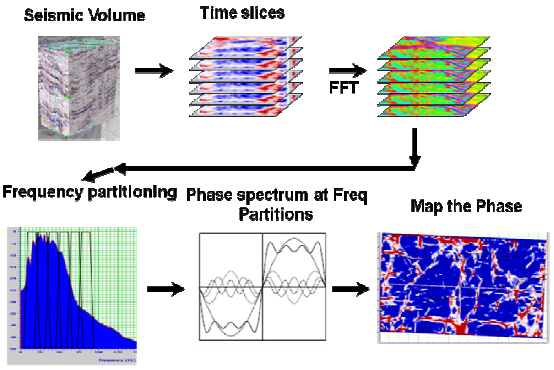

Figure 1. A schematic showing the implementation of the phase congruency algorithm to seismic data.

Example

We will apply the phase congruency algorithm to a 3D dataset over a Karst collapse feature from the Boonsville area of north Texas. The wells and 3D seismic from this dataset are public domain, and available from the Bureau of Economic Geology at the University of Texas. A map of the area is shown in Figure 2.

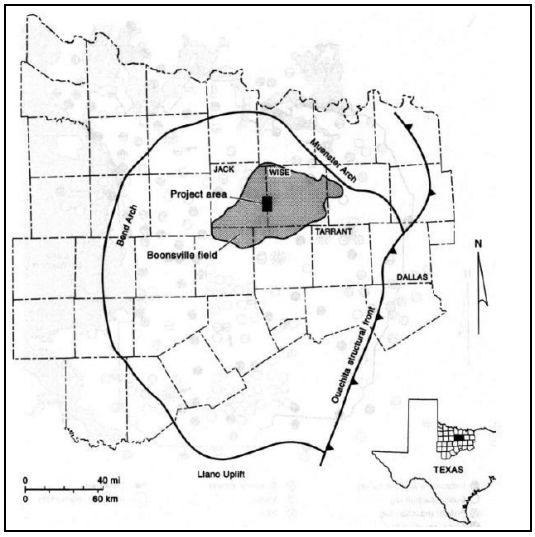

Figure 2. A map showing the location of the Boonsville gas field. (Hardage et al., 1996).

The geology of the area and exploration objectives of the Boonsville dataset has been fully described by Hardage et al. (1996). To illustrate the geology, a representative seismic section from this paper is shown in Figure 3.

In the Boonsville gas field, production is from the Bend conglomerate, a middle Pennsylvanian clastic deposited in a fluvio-deltaic environment. In Figure 3, the top of the Bend formation is indicated by event 1 at 850 ms, the Caddo, and the base of the Bend is indicated by event 4 at 1050 ms, the Vineyard. The Bend formation is underlain by Paleozoic carbonates, the deepest being the Ellenburger Group of Ordovician age. The Ellenburger contains numerous karst collapse features which extend up to 760 m from basement through the Bend conglomerate. As can be seen in Figure 3, these Karst collapse features, illustrated by the vertical ellipses, have a significant effect on the basal Vineyard event and continue vertically almost until the top Caddo event. Hardage et al. (1996) demonstrate, using measured pressure data, that these karst collapse features affect reservoir compartmentalization within the producing Bend formation.

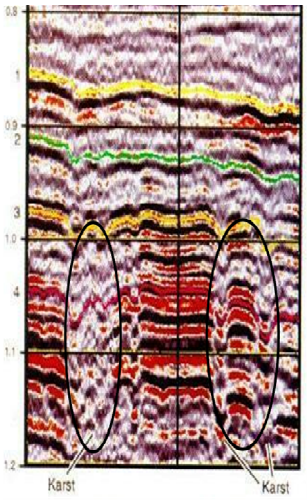

Figure 3. A representative seismic section from the 3D Boonsville dataset, with the producing horizons numbered from 1 to 4, and the Karst collapse features identified by the ellipses.

It is therefore important to identify the karst collapse features from the seismic volume, and we will do this using both the phase congruency and coherency methods. Figure 4 shows a set of composite slices (in the X, Y and Z directions) over the 3D seismic survey illustrated by the white outline in Figures 4(a) and (b), where Figure 4(a) shows the original seismic survey and Figure 4(b) shows the phase congruency results. On Figure 4(a), the Y-direction, or in-line, slice shows the karst features quite clearly (they are annotated with the red ellipses) but on the horizontal time slice they are not as clear. On Figure 4(b), the in-line slice shows the karst features even more clearly than on the seismic display (again, they are annotated with the red ellipses) and on the horizontal time slice they are also much clearer.

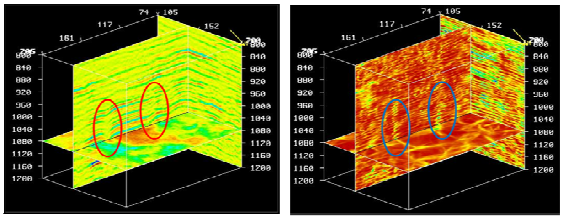

(a) (b)

Figure 4. A vertical slice showing karst features superimposed on a horizontal slice at 1080 ms, roughly halfway through the karst collapse, where (a) shows the seismic volume and (b) shows the phase congruency volume.

Figure 5 shows the same set of composite slices (in the X, Y and Z directions) as in Figure 4, where Figure 4(a) again shows the original seismic survey and Figure 4(b) now shows the coherency results.

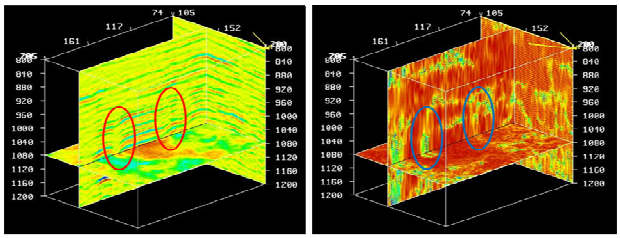

(a) (b)

Figure 5. A vertical slice showing karst features superimposed on a horizontal slice at 1080 ms, roughly halfway through the karst collapse, where (a) shows the seismic volume and (b) shows the coherency volume.

On Figure 5(b), the in-line slice shows the karst features more clearly than on the seismic display (again, they are annotated with the red ellipses) than on the seismic display, but slightly less clearly than on the phase coherency.

Conclusions

In this paper, we implemented a new scheme for identifying discontinuities on seismic data slices, called phase congruency. As we discussed, the phase congruency approach has found application in the identification of features on images and is used in image processing for robot vision. However, the method had found little application in the seismic area and so we decided to see if it could aid in the search for discontinuities on seismic time slices.

We first described the theory of the phase congruency method. We then applied the algorithm to a 3D seismic dataset. In this example, a karst collapse study from the Boonsville field in Texas, we found that phase congruency did a good job in identifying these karst features. From an economic standpoint, the identification of the karst features was of great interest since it lead to the identification of compartmentalization in the reservoir interval above the karst collapse zones.

References

Bahorich, M. and Farmer, S., 1995, 3-D seismic discontinuity for faults and stratigraphic features: The coherence cube: THE LEADING EDGE, 14, no. 10, 1053-1058.

Cook, J., Chandran, V. and Fookes, C., 2006, 3D face recognition using log-Gabor templates: presented at the British Machine Vision Conference (BMVC), September 4-7, 2006, Edinburgh.

Field, D., 1987, Relations between the statistics of natural images and the response properties of cortical cells: Journal of the Optical Society of America, vol. 4, no. 12, pp 2379-2394.

Hardage, B.A., Carr, D.L., Lancaster, D.E., Simmons, J.L. Jr., Elphick, R.Y., Pendleton, V.M. and Johns, R.A., 1987, 3-D seismic evidence of the effects of carbonate karst collapse on overlying clastic stratigraphy and reservoir compartmentalization, GEOPHYSICS, 61, 1336-1350.

Kovesi, P.D., 2003, Phase congruency detects corners and edges: Proceedings of the Seventh Australasian Conference on Digital Image Computing Techniques and Applications (DICTA'03).

Lucia, F.J., 1995, Lower Paleozoic cavern development, collapse and dolomitization, Franklin Mountains, El Paso, Texas, in Budd, D.A., Saller, A.H., and Harris, P.M., Eds., Unconformities and porosity in carbonate strata: AAPG Memoir 63, 279-300.

Acknowledgements

We wish to thank our colleagues at the CREWES Project, CGGVeritas and Talisman for their support and ideas, as well as the sponsors of the CREWES Project.